Numerical Investigation on flash boiling GDI spray collapse process using HRM model

Jingyu Zhang[1], Yanfei Li[1]*, Songzhi Yang[2], Hongming Xu[1], Shijin Shuai[2]
[1]State Key Laboratory of Automotive Safety and Energy, Tsinghua University, Beijing, 100084, China
[2]Institute for Aero Engine, Tsinghua University, Beijing, 100084, China

Abstract
Further investigation into the collapse mechanism of multi-jet flash boiling sprays is crucial to improve the mixture formation in gasoline direct injection (GDI) engines. Herein, n-hexane flash boiling sprays from a five-hole GDI injector have been numerically studied using the homogeneous relaxation model (HRM). The collapse process has been validated by the experimental data in terms of spray penetration length and spray width. For the given case, as the individual jets were discharged from the nozzle, they became under-expanded, where a typical shock structure (primary cell) can be well observed for each individual jets. Then, strong interactions were found between the adjacent jets leading to the formation of secondary cells. It was found the jet-to-jet structure did not form a closed ring, indicating that the closed-ring jet-to-jet structure might be not the necessity for the flash boiling spray collapse. The pressure distribution by two cross-sections revealed the low-pressure region development process and the shock structure vibration characteristic. The initial generation reason for the crown structure in the spray tip was considered the flow separation of the different near-field collapse levels in this process.

Keywords
Flashing boiling, Under-expanded jet, Spray collapse, Shock.

Introduction

Nowadays, gasoline direct injection (GDI) engines are the mainstream power source of passenger cars. Due to the high fuel volatility, the high injector temperature, and the relatively low ambient pressure during the fuel injection process, flash boiling has been found frequently in GDI engines [1]. Flash boiling is a phase transition that occurs when the liquid is suddenly exposed to an environment with pressure lower than its saturation point. Compared with the spray atomization obtained by mechanical means under equal injection pressure, flash boiling spray has exhibited improved atomization quality [2]. And the benefit of flash boiling has been mentioned to generate ideal sprays for GDI engines [3].

However, the flash boiling jets discharged from multi-hole injectors would contract to the spray axis and even merge into one jet. The above phenomenon is referred to spray collapse or contraction. Spray collapse could significantly change the mixture formation, might lead to adverse effects such as fuel-wall impingement [4]. The fuel-wall impingement was considered to be the significant source of soot formation [5]. To take full advantage of flash boiling injection, much research has been conducted on the spray collapse mechanism.

Heldmann et al. [6] proposed that the different pressure between ambient and spray center induce the spray collapse. Yang et al. [7] revealed that the adjacent plumes overlap enhance the spray collapse. A recent study indicated that the difference of spray collapse cause under flashing and non-flashing conditions [8]. The subcooled spray generally became collapse under high ambient pressure conditions due to the air entrainment causing and enhancing the central low-pressure zone [9, 10]. However, a recent study has considered that the massive

production of vapor counteracts the low-pressure tendency, explaining the cause of flash boiling spray collapse is different to the subcooled condition [11]. Lacey et al. [12] attributed the flash boiling spray collapse to the under-expanded flow rapid expansion and resulting plume-to-plume interaction when flow leaving the nozzle. Guo et al. [13-15] used the HRM model to reveal that due to the flow under-expansion, low-pressure regions were formed in flash boiling jets and sprays and the jet-to-jet interaction caused spray collapse. These results paid little attention to the formation process of the spray collapse.

The present study is the continuity of our previous studies [13, 14] and aims at analyzing the development process of spray collapse in the multi-jet flashing spray with experimental validation. Three-dimensional numerical simulations are carried out on the flash boiling spray of a five-hole GDI injector using the CFD software CONVERGE v3.0. This paper consists of two parts. In the first part, the spray morphology collapse process is validated by experimental data. In the second part, the jet-to-jet interaction development process is analysed in terms of shock structure and pressure distribution, which the correlation with the spray morphology is also discussed.

Methodology

- *Injector specifications and mesh strategy*

A five-hole commercial GDI injector was used in the simulation. The nozzle structure and the nozzle layout are shown in Figure **1**. The hole consists of an inner hole and a counterbore, as shown in the micrograph of the fractured injector tip **(**Figure **1 (c)**). The diameters of the inner hole and the counterbore are 0.18 mm and 0.46 mm, respectively. And the lengths of the inner hole and the counterbore are 0.16 mm and 0.42 mm, respectively. The nozzle layout and the hole structure was captured by serial layer scanning X-ray and established in the CFD software, as shown in Figure **2** (a) and (b)**.**

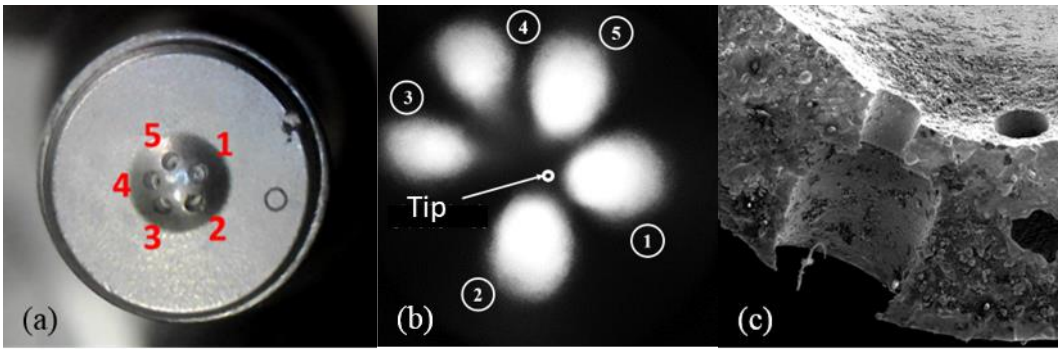

Figure 1. The injector condition: (a) nozzle layout, (b) jets drop pattern, (c) hole structure.

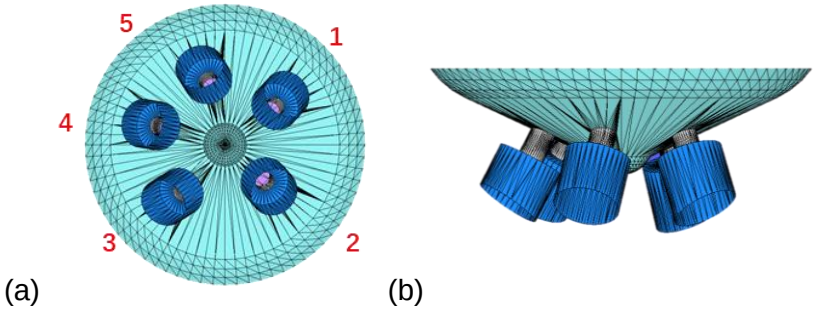

Figure 2. The CFD injector geometry: (a) bottle view ,(b) side view of injector geometry in CFD.

The base grid size in the computational domain was 800 μm. Fixed embedded refinement with a grid size of 12.5 μm was used to discretize the orifice region, which corresponding 6 level embedding scale. The grid size of 25 μm was used to discretize the inner-injector regions,

which corresponding to 5 level embedding scale. The grid size of 100 μm was used to discretize the spray encircle cone regions, which corresponding to 3 level embedding scale. In all regions, adaptive mesh refinement (AMR) was applied to achieve an appropriate accuracy based on the velocity, temperature, and void fraction, which can embed up to a minimum grid size of 12.5 μm with 6 level. Except for providing the necessary mesh resolution, the application of AMR allowed for the correct capture of a shock structure, as shown in Figure **3**. The grid control strategy was chosen based on a previous study [14], which reported that a minimum mesh size of 12.5 μm is sufficient to capture shock in flash boiling sprays. To balance the accuracy and consumption, the maximum cell count was limited to 30 million.

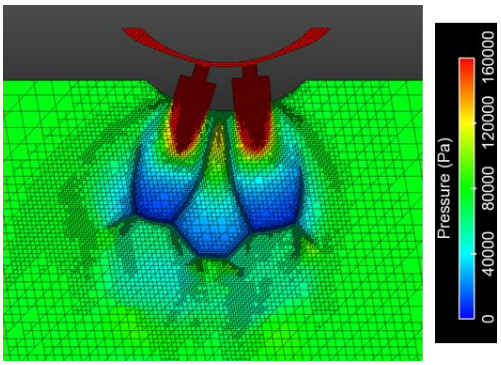

Figure 3. A slice of mesh generated at the quasi-steady state: shock captured with the application of AMR in the section through the center of hole 4 and 5.

- *Physical models and numerical setup*

The simulation in this work relied on a Reynolds-Averaged Navier-Stokes (RANS) formulation closed by the RNG k-ε model. The simulation used the one-fluid model, which solved one set of governing equations. The two-phase mixture was assumed as a pseudo fluid, whose physical properties were calculated using the interpolation method. The liquid and gaseous phases were simulated as compressible. The liquid density was defined as a barotropic function of the local mixture pressure. And the Redlich-Kwong equation was used for the gaseous phase properties calculation. A detailed description of the governing equations can be found in a previous study [13].

The homogeneous relaxation model (HRM) proposed by Bilicki and Kestin[16] was used to determine the mass exchange between the liquid and vapor due to flash boiling. The HRM model describes the evolution of the instantaneous vapor quality utilizing a first-order relaxation towards the equilibrium value over a time scale. In the HRM model, the rate of phase transition is described as:

$$\frac{Dx}{Dt} = \frac{\bar{x} - x}{\theta} \tag{1}$$

Where x represents the instantaneous mass. $\bar{x}$ represents the equilibrium mass and θ represents the time scale over which x relaxes to $\bar{x}$. For evaporation, the time scale θ_E can be represented as follows:

$$\theta_E = \theta_0 \alpha^{-0.54} \frac{P_{sat} - P}{P_c - P_{sat}}^{-1.76} \tag{2}$$

where α is the void fraction, P_c is the critical pressure, P is the instantaneous pressure, P_{sat} is the saturation pressure. The value of the coefficient θ_0 was chosen as 1e-9 s, according to the previous simulation study of n-hexane flash boiling spray [14].

The simulation duration time was 100 μs, which was chosen to ensure that the quasi-steady-state of the near-nozzle flow has been reached. Initially, the upstream region of the inner hole was filled with liquid fuel at the injection temperature and pressure. In contrast, the nozzle and chamber were filled with nitrogen at ambient temperature and pressure. During the simulation, liquid fuel entered the domain from the inlet boundary with constant injection pressure and temperature values. Constant ambient pressure was applied at the outlet boundary. A variable time-step was used, controlled by a convection Courant-Friedrichs-Lewy (CFL) number of 0.25 and a Mach-based CFL number of 5.0. A modified pressure implicit splitting of operators (PISO) method [17] was used to couple pressure and velocity. The commercial code CONVERGE v3.0 was chosen.

- *Operating condition*

N-hexane was used as the injection fluid, representing a mono-component surrogate of gasoline under flash boiling conditions [18]. The injection pressure was set as 10.0MPa. The ambient pressure was set as 80kPa, and the ambient temperature was set as 300K. The injection temperature was set as 393K, corresponding to the superheat degree (R_p) of 4.83, which was the ratio of the saturation pressure(P_{sat}) at the injection temperature (T_{inj}) to the ambient pressure (P_{amb}). Besides, the needle lift was set as 50μm, which the raising process of the needle was not considered.

- *Experimental setup*

The high-speed imaging technique was employed to acquire the spray morphology. The n-hexane spray process in a constant volume vessel was captured under the same condition with simulation. And the spray morphology was acquired by a uniform backlight, implying that the image darkness represents spray droplet concentration. A detailed description of the experimental methodology can be found in a previous study [19]. In this research, high-speed camera FASTCAM SA-Z was set with the 100,000fps shooting speed, 1/6,300,000s shutter, 384x256pixels resolution. The final spray morphology was an average of 10 repeated injections.

Results and Discussion

- *Spray morphology and validation*

The high injection pressure in the GDI engine resulted in a high mass flow rate, and a high optical thickness, which meant the shock structure inside the spray was hardly captured using an optical technique. Thus, to validate the simulation results, the consistency in some morphology features between experiment and simulation would be explained in the following. Figure **4 (a)** and **(b)** show the development process of experiment and simulation spray morphology, indicating a high degree of agreement on the whole, especially in the relatively stable state (after 0.07 ms). It is noted that the iso-surface of the 5% liquid mass fraction was used to represent the spray boundary in the simulation. A crown structure in the spray tip as a typical feature of flash-boiling collapse spray was observed in experiments and simulations. And the development process of the spray penetration length between simulation and experiment demonstrated a high degree of consistency, as shown in Figure **5 (a)**. The process of obtaining the penetration length and spray width from the experiment and simulation images can be seen in Figure **5 (b)** and **(c)**. For more details about image processing, please refer to our previous research[20]. The penetration length remained stable after 0.75 ms ASOI because the spray tip had reached the simulation domain boundary and the experimental view field, respectively. And for the experimental results, since the data resolution is at 0.01ms, the

development process of the spray penetration between 0.07 ~ 0.08ms has slowed down. In the early stage of spray, the penetration length in the experiment was less than the simulation result because the establishment of fuel pressure in the real injector would take a certain amount of time. However, the penetration length between the simulation and experiment tends to become consistent after the establishment of the fuel pressure in the real injector.

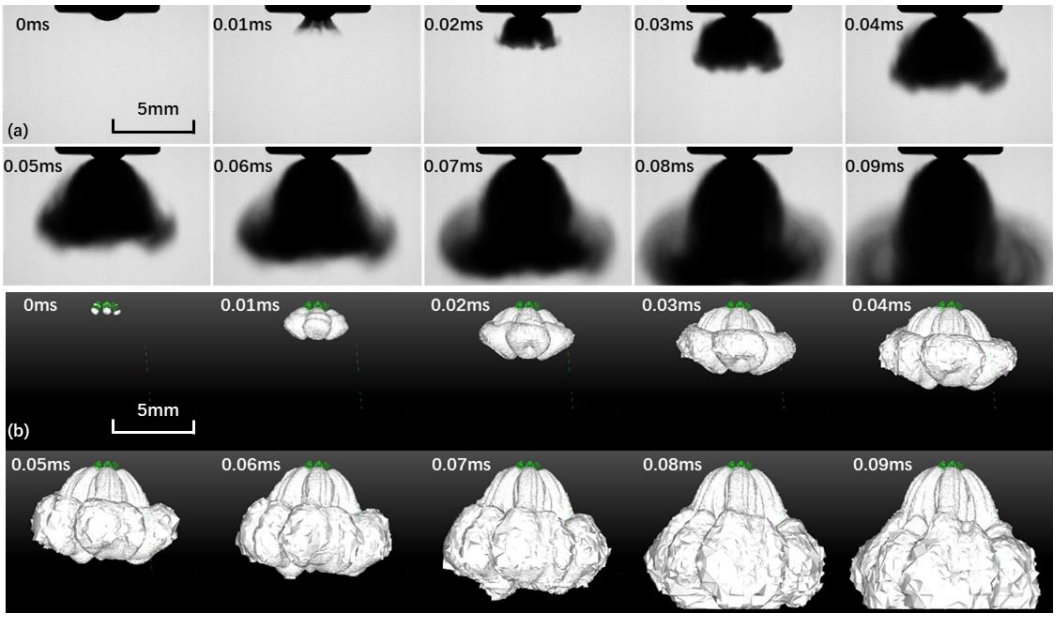

Figure 4. The development process of (a) experimental spray morphology, (b) the iso-surface of the 5% liquid mass fraction in the simulated spray.

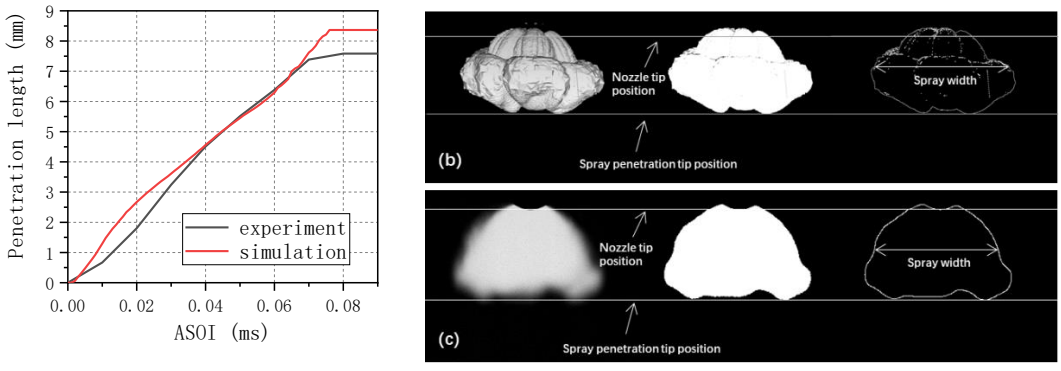

(a)

Figure 5. The spray penetration length: (a) the development process, (b) the image processing in the simulation, (c) the image processing in the experiment.

The formation process of spray collapse could be roughly divided into two stages of morphology, according to experiment and simulation, simultaneously. In the first stage, the near-field collapse was gradually formed and strengthened, as shown in Figure **4 (a)** and **(b)** 0.01 ~ 0.06 ms. At the start of injection (such as 0.01 ms), the near-field spray did not show significant collapse. Then, the near-field collapse gradually strengthened with the spray developing, which could be observed through the spray width in Figure **6 (a)** and **(b)** 0.04 ~ 0.06 ms. In the second stage, the near-field collapse remained stable, as shown in Figure **6 (a)** and **(b)** 0.08 and 0.09 ms. The upstream region of the crown structure had entered a relatively stable collapse state, in this stage.

It could be found the simulation spray morphology generally matched well with the experiment result in terms of spray penetration length and spray width, demonstrating the validity of the model.

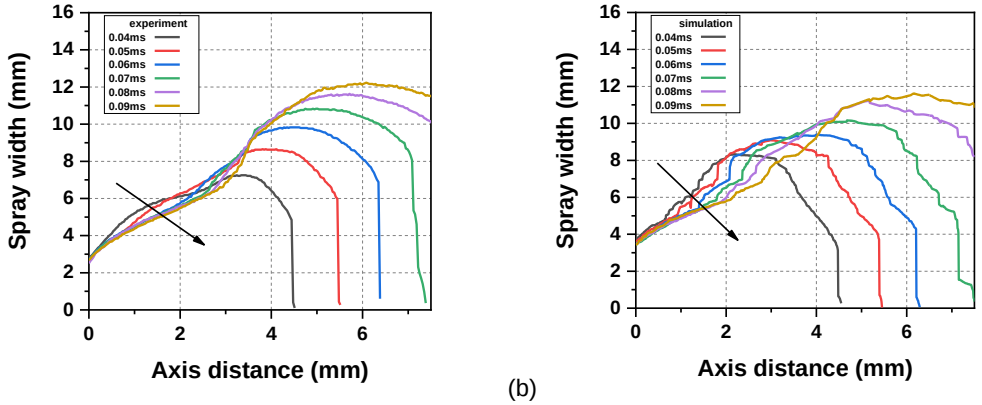

(a) (b)

Figure 6. The spatial-resolved spray width at a certain time: (a) the experiment, (b) the iso-surface of the 5% liquid mass fraction in the simulated spray.

- *Jet-to-jet interaction*

Figure **7** shows the iso-surface of Mach number equalling 1 in the simulation from side view and bottom view, representing the shock structure inside the spray. Once the injection started, supersonic flow and the primary shock of each jet appeared. Initially, the primary cells were formed and gradually developed, as shown in Figure **7 (a)** and **(b)** 0.01 ms. Then, the Mach disk appeared with primary cells developing, and secondary cells between adjacent primary cells were formed, as shown in Figure **7 (a)** and **(b)** 0.02 ms. The jets became under-expanded. Finally, the shock structure entered a relatively stable state, as shown in Figure **7 (b)** 0.06 ~ 0.09 ms.

For the given case, the interaction only existed between adjacent jets. In other words, no direct interaction was found between non-adjacent jets. Under the effect of low-pressure region inside single jet and between adjacent jets, the flash boiling spray became collapse, which was consistent with other studies [15]. However, Figure **7 (b)** shows that there was no interaction between a couple of adjacent jets (jet 2 and 3), explaining the jet-to-jet interactions did not form a closed ring. The comparison of the pressure distribution between interaction (jet 1 and 5) and non-interaction (jet 2 and 3) of adjacent jets could be clearly observed in Figure 9 **(b)**. Furthermore, the closed-ring jet-to-jet structure might be not the necessity for the flash boiling spray collapse.

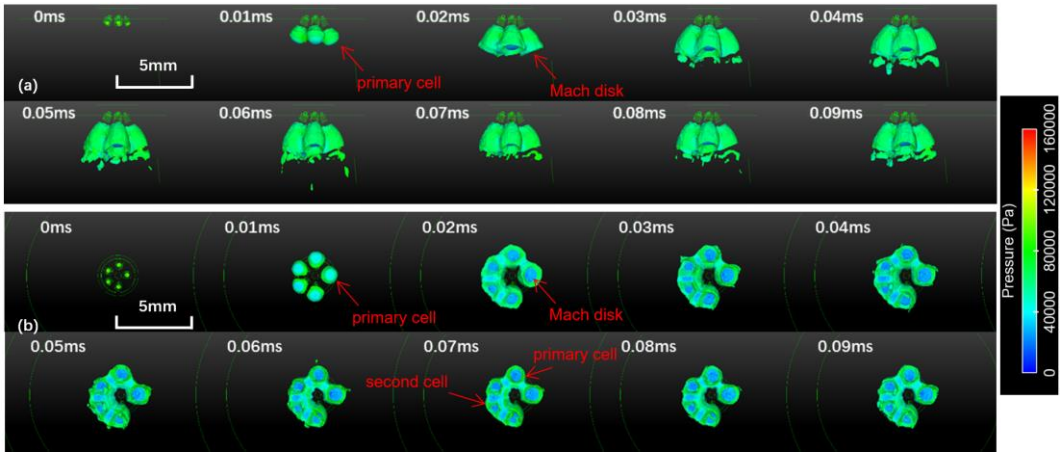

Figure 7. The development process of the iso-surface of Mach number equalling 1: (a) side view, (b) bottom view.

Two cross-sections were selected to better understand the pressure distribution inside the shock structure, as shown in Figure 8. Section A was through the center of jet 4 and 5, representing the situation between adjacent jets. Section B was through the bisector of jet 1 and 5, describing the situation between adjacent jets in the spray radial direction.

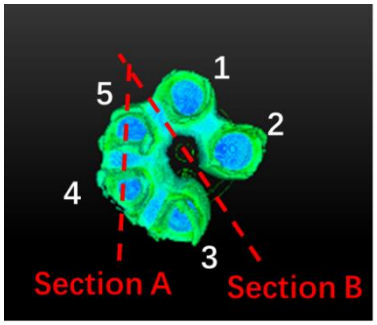

Figure 8. The schematic of the section.

Figure 9 shows the temporal evolution of pressure in the above two cross-sections. It needed to be pointed out that the discontinuity line of pressure meant the shock surface and corresponded to iso-surface of Mach number equalling 1 in Figure 7. The low-pressure regions inside primary cells and second cells were considered an essential cause of spray collapse [15].

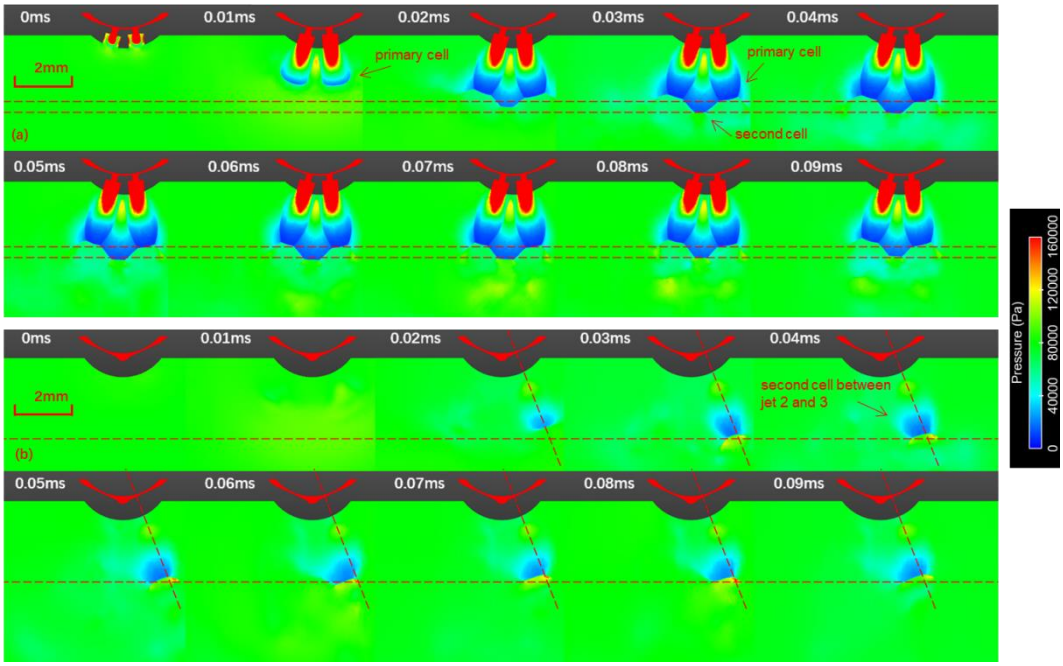

Figure 9. Temporal evolution of pressure in (a) Section A, (b) Section B.

For adjacent jets, Figure 9 **(a)** shows the development process of the primary cell (0 ~ 0.03 ms) and second cell (0.01 ~ 0.03 ms) from emergence to stability. And under the developing process before relative stability (0 ~ 0.02 ms), the area and strength of low-pressure regions inside and between the jets were weaker than the stability state from Figure 9 **(a)**, explaining the reason why the near-field spray collapse was no sign at the start of injection. A vibration characteristic for second cells was observed in radial and circumferential directions from Figure 9 **(a)** and **(b)**. In particular, a period of vibration might exist between 0.03 ~ 0.09 ms. The vibration characteristics will not be discussed further in this study, and we regard it as a relatively stable state.

It took about 0.03 ms for the shock structure to fully develop and reach relatively stability, in this case. The near-field spray collapse was gradually enhancing in the process of shock structure developing. The crown structure forms as the near-field spray collapse is not fully formed when the fuel leaving the nozzle. These fuel continue moving downstream in a non-collapse trend by their inertia and is spatially deflected from the other fuel leaving the nozzle when the near-field spray collapse has arrived the stable point. It is confimed that the behavior of the crown structure is the combined effects of many factors (such as the gas entrainment, the flow resistance); here is just to discuss the initial reason for its generation.

Conclusions

In this study, the collapse process of n-hexane flash boiling sprays from a five-hole GDI injector was studied numerically. The process of spray collapse caused by the low-pressure region was discussed in detail to understand the collapse mechanism further. The conclusive remarks are as follows.

1) The simulation spray morphology generally matched well with the experiment result in spray penetration length and spray width development process, demonstrating the effectivity of the HRM model.

2) The interaction only exists between adjacent jets in this case. The spray collapse still occurred under a couple of adjacent jets without interaction, indicating that the closed-ring jet-to-jet structure might not be necessary for the flash boiling spray collapse.

3) The process of shock structure fully developing and reaching relatively stability took about 0.03 ms, in this case. The initial generation reason for the crown structure in the spray tip was considered the flow separation of the different near-field collapse levels in this process.

Acknowledgments

It is financially supported by National Science Foundation of China under Grant NO. 52076119.

Nomenclature

GDI Gasoline direct injection

ASOI After start of injection

References

[1] Kramer, M., Kull, E., and Wensing, M., 2016, "Flashboiling-induced targeting changes in gasoline direct injection sprays," International Journal of Engine Research, 17(1), pp. 97-107.

[2] Sher, E., Bar-Kohany, T., and Rashkovan, A., 2008, "Flash-boiling atomization," Progress in Energy and Combustion Science, 34(4), pp. 417-439.

[3] Xu, M., Zhang, Y., Zeng, W., Zhang, G., and Zhang, M., 2013, "Flash Boiling: Easy and Better Way to Generate Ideal Sprays than the High Injection Pressure," SAE International.

[4] Guo, H., Ma, X., Li, Y., Liang, S., Wang, Z., Xu, H., and Wang, J., 2017, "Effect of flash boiling on microscopic and macroscopic spray characteristics in optical GDI engine," Fuel, 190, pp. 79-89.

[5] Wang, B., Mosbach, S., Schmutzhard, S., Shuai, S., Huang, Y., and Kraft, M., 2016, "Modelling soot formation from wall films in a gasoline direct injection engine using a detailed population balance model," Applied Energy, 163.

[6] Heldmann, M., Bornschlegel, S., and Wensing, M., 2015, "Investigation of Jet-to-Jet Interaction in Sprays for DISI Engines," SAE Technical Paper Series, SAE International.

[7] Yang, S., Song, Z., Wang, T., and Yao, Z., 2013, "AN EXPERIMENT STUDY ON PHENOMENON AND MECHANISM OF FLASH BOILING SPRAY FROM A MULTI-HOLE GASOLINE DIRECT INJECTOR," Atomization and Sprays, 23(5), pp. 379-399.

[8] Guo, H., Ding, H., Li, Y., Ma, X., Wang, Z., Xu, H., and Wang, J., 2017, "Comparison of spray collapses at elevated ambient pressure and flash boiling conditions using multi-hole gasoline direct injector," Fuel, 199, pp. 125-134.

[9] Khan, M., Helie, J., Gorokhovski, M., and Sheikh, N., 2017, "Air Entrainment in High Pressure Multihole Gasoline Direct Injection Sprays," Journal of Applied Fluid Mechanics, 10, pp. 1223-1234.

[10] Sphicas, P., Pickett, L. M., Skeen, S. A., and Frank, J. H., 2018, "Inter-plume aerodynamics for gasoline spray collapse," International Journal of Engine Research, 19(10), pp. 1048-1067.

[11] Guo, H., Li, Y., Shen, Y., Zhang, Z., Ma, X., Xu, H., and Wang, Z., 2018, "Characterizing Propane Flash Boiling Spray from Multi-Hole GDI Injector," SAE Technical Paper Series, SAE International.

[12] Lacey, J., Poursadegh, F., Brear, M. J., Gordon, R., Petersen, P., Lakey, C., Butcher, B., and Ryan, S., 2017, "Generalizing the behavior of flash-boiling, plume interaction and spray collapse for multi-hole, direct injection," Fuel, 200, pp. 345-356.
[13] Guo, H., Li, Y., Wang, B., Zhang, H., and Xu, H., 2019, "Numerical investigation on flashing jet behaviors of single-hole GDI injector," International Journal of Heat and Mass Transfer, 130, pp. 50-59.
[14] Guo, H., Li, Y., Xu, H., Shuai, S., and Zhang, H., 2019, "Interaction between under-expanded flashing jets: A numerical study," International Journal of Heat and Mass Transfer, 137, pp. 990-1000.
[15] Guo, H., Nocivelli, L., and Torelli, R., 2021, "Numerical study on spray collapse process of ECN spray G injector under flash boiling conditions," Fuel, 290, p. 119961.
[16] Bilicki, Z., Kestin, J., and Stuart, J. T., 1990, "Physical aspects of the relaxation model in two-phase flow," Proceedings of the Royal Society of London. A. Mathematical and Physical Sciences, 428(1875), pp. 379-397.
[17] Issa, R. I., 1986, "Solution of the implicitly discretised fluid flow equations by operator-splitting," Journal of Computational Physics, 62(1), pp. 40-65.
[18] Araneo, L., and Donde, R., 2017, "Flash boiling in a multihole G-DI injector – Effects of the fuel distillation curve," Fuel, 191, pp. 500-510.
[19] Li, Y., Guo, H., Zhou, Z., Zhang, Z., Ma, X., and Chen, L., 2019, "Spray morphology transformation of propane, n-hexane and iso-octane under flash-boiling conditions," Fuel, 236, pp. 677-685.
[20] Li, Y., Guo, H., Ma, X., Qi, Y., Wang, Z., Xu, H., and Shuai, S., 2018, "Morphology analysis on multi-jet flash-boiling sprays under wide ambient pressures," Fuel, 211, pp. 38-47.